

Casting method for producing low-loss chalcogenide microstructured optical fibers

Quentin Coulombier¹, Laurent Brilland^{2,*}, Patrick Houizot¹, Thierry Chartier³, Thanh Nam N'Guyen³, Frédéric Smektala⁴, Gilles Renversez⁵, Achille Monteville², David Méchin², Thierry Pain¹, Hervé Orain⁶, Jean-Christophe Sangleboeuf⁶, Johann Trolès¹

¹ UMR CNRS 6226, Equipe Verres et Céramiques, Campus de Beaulieu, 35042 Rennes Cedex, France

² PERFOS, 11, Rue Louis de Broglie 22300 Lannion, France

³ ENSSAT, 6 rue de Kerampont, BP 80518, 22305 Lannion Cedex, France

⁴ Laboratoire Interdisciplinaire Carnot de Bourgogne, UMR 5209 CNRS-Université de Bourgogne, 9 Av. A. Savary, BP 47870, 21078 DIJON Cedex, France

⁵ Institut Fresnel, UMR CNRS 6133, Université d'Aix-Marseille, 13397Marseille Cedex 20, France

⁶ LARMAUR, Campus de Beaulieu, 35042 Rennes Cedex, France
*lbrilland@perfos.com

Abstract: We report significant advances in the fabrication of low loss chalcogenide microstructured optical fiber (MOF). This new method, consisting in molding the glass in a silica cast made of capillaries and capillary guides, allows the development of various designs of fibers, such as suspended core, large core or small core MOFs. After removing the cast in a hydrofluoric acid bath, the preform is drawn and the design is controlled using a system applying differential pressure in the holes. Fiber losses, which are the lowest recorded so far for selenium based MOFs, are equal to the material losses, meaning that the process has no effect on the glass quality.

©2010 Optical Society of America

OCIS codes: (060.2390) Fiber optics, infrared; (190.4370) Nonlinear optics, fibers; (060.5295) Photonic crystal fibers.

References and links

1. J. S. Sanghera, C. M. Florea, L. B. Shaw, P. Pureza, V. Q. Nguyen, M. Bashkansky, Z. Dutton, and I. D. Aggarwal, "Non-linear properties of chalcogenide glasses and fibers," *J. Non-Cryst. Solids* **354**(2-9), 462–467 (2008).
2. L. Petit, N. Carlie, K. Richardson, A. Humeau, S. Cherukulappurath, and G. Boudebs, "Nonlinear optical properties of glasses in the system Ge/Ga-Sb-S/Se," *Opt. Lett.* **31**(10), 1495–1497 (2006).
3. T. M. Monro, Y. D. West, D. W. Hewak, N. G. R. Broderick, and D. J. Richardson, "Chalcogenide holey fibres," *Electron. Lett.* **36**(24), 1998–2000 (2000).
4. J. S. Sanghera, I. D. Aggarwal, L. B. Shaw, C. M. Florea, and P. Pureza, V. Q. NGuyen, F. Kung, and I. D. Aggarwal, "Nonlinear properties of chalcogenide glass fibers," *J. Optoelectron. Adv. Mat.* **8**, 2148–2155 (2006).
5. L. Brilland, F. Smektala, G. Renversez, T. Chartier, J. Trolès, T. Nguyen, N. Traynor, and A. Monteville, "Fabrication of complex structures of Holey Fibers in Chalcogenide glass," *Opt. Express* **14**(3), 1280–1285 (2006).
6. F. Désévéday, G. Renversez, L. Brilland, P. Houizot, J. Trolès, Q. Coulombier, F. Smektala, N. Traynor, and J.-L. Adam, "Small-core chalcogenide microstructured fibers for the infrared," *Appl. Opt.* **47**(32), 6014–6021 (2008).
7. F. Désévéday, G. Renversez, J. Trolès, L. Brilland, P. Houizot, Q. Coulombier, F. Smektala, N. Traynor, and J.-L. Adam, "Te-As-Se glass microstructured optical fiber for the middle infrared," *Appl. Opt.* **48**(19), 3860–3865 (2009).
8. G. Renversez, B. Kuhlmeier, and R. McPhedran, "Dispersion management with microstructured optical fibers: ultraflattened chromatic dispersion with low losses," *Opt. Lett.* **28**(12), 989–991 (2003).
9. B. Temelkuran, S. D. Hart, G. Benoit, J. D. Joannopoulos, and Y. Fink, "Wavelength-scalable hollow optical fibres with large photonic bandgaps for CO₂ laser transmission," *Nature* **420**(6916), 650–653 (2002).

10. C. V. M. Fridlund, "Darwin – The Infrared Space Interferometry Mission," *ESA Bull.* **103**, (2000).
11. E. Austin, A. van Brakel, M. N. Petrovich, and D. J. Richardson, "Fibre optical sensor for C₂H₂ gas using gas-filled photonic bandgap fibre reference cell," *Sens. Actuators B Chem.* **139**(1), 30–34 (2009).
12. F. Charpentier, J. Troles, Q. Coulombier, L. Brilland, P. Houizot, F. Smektala, and P. Boussard, C. del, V. Nazabal, N. Thibaud, K. Le Pierres, G. Renversez, and B. Bureau, "CO₂ Detection Using Microstructured Chalcogenide Fibers," *Sensor Letters* **7**, 745–749 (2009).
13. C. Fortier, J. Fatome, S. Pitois, F. Smektala, G. Millot, J. Troles, F. Desevedavy, P. Houizot, L. Brilland, and N. Traynor, "Experimental investigation of Brillouin and Raman scattering in a 2SG sulfide glass microstructured chalcogenide fiber," *Opt. Express* **16**(13), 9398–9404 (2008).
14. J. M. Dudley, G. Genty, and S. Coen, "Supercontinuum generation in photonic crystal fiber," *Rev. Mod. Phys.* **78**(4), 1135–1184 (2006).
15. V. G. Ta'eed, M. Shokooh-Saremi, L. Fu, I. C. M. Littler, D. J. Moss, M. Rochette, B. J. Eggleton, R. Yinlan, and B. Luther-Davies, "Self-phase modulation-based integrated optical regeneration in chalcogenide waveguides," *IEEE J. Sel. Top. Quant. Electron.* **12**(3), 360–370 (2006).
16. L. Fu, M. Rochette, V. Ta'eed, D. Moss, and B. Eggleton, "Investigation of self-phase modulation based optical regeneration in single mode As₂Se₃ chalcogenide glass fiber," *Opt. Express* **13**(19), 7637–7644 (2005).
17. J. C. Knight, T. A. Birks, P. S. J. Russell, and D. M. Atkin, "All-silica single-mode optical fiber with photonic crystal cladding," *Opt. Lett.* **21**(19), 1547–1549 (1996).
18. M. Liao, C. Chaudhari, G. Qin, X. Yan, C. Kito, T. Suzuki, Y. Ohishi, M. Matsumoto, and T. Misumi, "Fabrication and characterization of a chalcogenide-tellurite composite microstructure fiber with high nonlinearity," *Opt. Express* **17**(24), 21608–21614 (2009).
19. L. Brilland, J. Troles, P. Houizot, F. Desevedavy, Q. Coulombier, G. Renversez, T. Chartier, T. N. Nguyen, J.-L. Adam, and N. Traynor, "Interfaces impact on the transmission of chalcogenides photonic crystal fibres (Glass and Ceramic Materials for Photonics)," *J. Ceram. Soc. Jpn.* **116**(1358), 1024–1027 (2008).
20. Y. Zhang, K. Li, L. Wang, L. Ren, W. Zhao, R. Miao, M. C. J. Large, and M. A. van Eijkelenborg, "Casting preforms for microstructured polymer optical fibre fabrication," *Opt. Express* **14**(12), 5541–5547 (2006).
21. Z. Guiyao, H. Zhiyun, L. Shuguang, and H. Lantian, "Fabrication of glass photonic crystal fibers with a die-cast process," *Appl. Opt.* **45**(18), 4433–4436 (2006).
22. D. Ležal, J. Pedlířková, J. Gurovič, and R. Vogt, "The preparation of chalcogenide glasses in chlorine reactive atmosphere," *Ceramics Silikaty* **40** (1996).
23. M. F. Churbanov, I. V. Scripachev, G. E. Snopatin, V. S. Shiryaev, and V. G. Plotnichenko, "High-Purity Glasses Based on Arsenic Chalcogenides," *J. Optoelectron. Adv. Mat.* **3**, 341–349 (2001).
24. J. S. Sanghera, and I. D. Aggarwal, "Active and passive chalcogenide glass optical fibers for IR applications: a review," *J. Non-Cryst. Solids* **256–257**, 6–16 (1999).
25. E. Thomson, "The mechanical, thermal and optical properties of fused silica," *J. Franklin Inst.* **200**(3), 313–326 (1925).
26. E. Guillevic, X. Zhang, T. Pain, L. Calvez, J.-L. Adam, J. Lucas, M. Guilloux-Viry, S. Ollivier, and G. Gadret, "Optimization of chalcogenide glass in the As-Se-S system for automotive applications," *Opt. Mater.* **31**(11), 1688–1692 (2009).
27. G. Renversez, F. Bordas, and B. T. Kuhlmei, "Second mode transition in microstructured optical fibers: determination of the critical geometrical parameter and study of the matrix refractive index and effects of cladding size," *Opt. Lett.* **30**(11), 1264–1266 (2005).
28. J. Troles, L. Brilland, F. Smektala, P. Houizot, F. Désévédy, Q. Coulombier, N. Traynor, T. Chartier, T. N. Nguyen, J. L. Adam, and G. Renversez, "Chalcogenide Microstructured Fibers for Infrared Systems, Elaboration Modelization, and Characterization," *Fiber Integrated Opt.* **28**(1), 11–26 (2009).
29. K. Ogusu, Y. Hosokawa, S. Maeda, M. Minakata, and H. Li, "Photo-oxidation of As₂Se₃, Ag-As₂Se₃, and Cu-As₂Se₃ chalcogenide films," *J. Non-Cryst. Solids* **351**(37-39), 3132–3138 (2005).
30. K. Ogusu, T. Hagihara, Y. Hosokawa, and M. Minakata, "Dependence of photo-oxidation on Ag(Cu)-content in Ag(Cu)-As₂Se₃ films," *J. Non-Cryst. Solids* **353**(11-12), 1216–1220 (2007).

1. Introduction

Chalcogenide glasses can be transparent from the visible region (sulfur based glass) up to the mid infrared (25 μm for telluride glasses). Another remarkable property of chalcogenide glasses is their strong optical nonlinearity. The nonlinear refractive index of sulfur based glasses is over 100 times higher than in silica and even 1000 times higher for selenium and tellurium based glasses [1, 2]. Another crucial advantage of chalcogenide glasses is the possibility to draw them into optical fibers as it has been demonstrated during the last 10 years. The first chalcogenide microstructured optical fiber (MOF) was reported in 2000 [3], but the fabricated suspended core MOFs did not show any light guidance. Since then, several chalcogenide MOFs with acceptable losses have been demonstrated for different core diameter [4–7].

MOFs, made of chalcogenide or other materials, have very specific optical properties. Depending on the design, they can be endlessly single-mode or single-mode with a very large mode area. Their geometric profiles can be modified to manage their chromatic dispersion [8]. The optical applications of chalcogenide MOFs are various. Depending on fiber design, chalcogenide MOFs can be used for power delivery [9], nulling interferometry for space-based applications [10] and pollutant detection or optical sensors [11,12]. Furthermore, the microstructured design can enhance the nonlinear optical properties of chalcogenide glasses to realize applications based on Brillouin and Raman scatterings [13], to generate supercontinuum sources [14] or even to build self-phase modulation based regenerator for telecommunication signals [15,16].

The common method to realize MOFs is the stack and draw technique which is widely used to make silica fibers [17] and chalcogenide MOFs [3, 4, 6, 18]. The lowest optical losses recorded so far for selenium based MOFs is 13 dB/m at 1.55 μm [6] and about 9 dB/m at 3.39 μm [7] using bulk material having only a few dB/m loss. In 2008, we have shown that most of the optical losses are due to inhomogeneities at the interfaces between capillaries [19]. Indeed, bubbles and crystals grow on the surface of chalcogenide capillaries and we have found that the transmission was greatly improved by using a fiber design including interstitial holes. However, the lowest losses obtained using this technique were still between 3 and 9 dB/m for selenium based glasses [19]. According to these results, it seems that the stack and draw method is not well suited to fabricate low loss chalcogenide MOFs which still remains a challenge.

In this paper, we describe an original method to realize chalcogenide MOFs of several types, included fibers with a suspended core design. This method based on casting allows us to increase considerably the transmission as inhomogeneities at the interfaces are greatly reduced. In 2006, Zhang et al. [20] and Guiyao et al. [21] showed respectively a similar method for making polymer and SF₆ glass MOFs. They used a mould which can be removed by heating or cooling the preform (or the metallic cast). They exploit the difference of thermal expansion between the mould and the preform to remove the cast. In our case, due to a large difference of thermal expansion properties, a metallic mould is not easily removable out of a chalcogenide glass. In this paper, we solved this problem by pouring chalcogenide glass into a silica mould. Using this technique, we have successfully removed the silica rods used to define the microstructure. For this study, the As₂Se₃ glass has been chosen for its high nonlinear refractive index and its low attenuation in mid-IR.

This article is organized as follows. In section 2, the preform and fiber fabrications are described. The optical characterization of the fabricated bulk glass and of the MOF are given and compared in section 3. Our results are discussed in section 4.

2. Preform and fiber fabrication

2.1 Principle

Glass rods are fabricated and purified with the usual sealed silica tube method. The As₂Se₃ glass is purified using oxygen and hydrogen getters such as TeCl₄ [22, 23] and Al. The losses are close to the lowest values recorded so far for these glasses [24]. Once the glass rod is synthesized, it is heated to become almost liquid but it must remain soft enough to flow on a silica mould. When the glass is in the mould, the tube is quenched in air and annealed. The silica structure is then removed with hydrofluoric acid before fiber drawing.

2.2 Preform fabrication

The mould is entirely made of silica capillaries thread in silica hexagonal guides (Fig. 1). The silica guides are slices of a silica microstructured preform. The hole diameter is 610 μm and the pitch is 1350 μm . The silica slices are fused in a silica tube (16 mm inner diameter, 5 cm between the slices) which is closed afterward. This arrangement allows the glass and the

capillaries to resist to mechanical stress induced by air quenching. Initially, the silica capillaries have an outer diameter of 600 μm and an inner diameter of approximately 490 μm . The diameter of the capillaries is reduced in a hydrofluoric acid (HF) bath to reach the outer diameter of 510 μm . The As_2Se_3 glass rod is placed above the mould, heated to 420 $^\circ\text{C}$ during one hour and poured into the mould in 5 minutes in a rocking furnace. It stays in vertical position for 15 minutes. The full mould is then quenched in air for four minutes before being annealed at 180 $^\circ\text{C}$ for one hour. After the silica tube is removed with a diamond tool. The structured As_2Se_3 preform is then treated with 40% concentrated HF in order to remove the silica capillaries stuck in the glass. After staying in the bath for one hour, the preform is rinsed with distilled water and dried with an argon purge.

2.3 Fiber fabrication

A glass drop appears when the heated preform falls down under gravitational forces forming a glass fiber which is then reeled on a drum in rotary motion. At the same time, the preform is moved down, feeding the drawing furnace. For a given feed speed of the preform, the diameter of the fiber is controlled by the drum speed. A narrow (5 mm width) drawing furnace is used to decrease the time during which the glass is in the critical high-temperature zone. A He gas flow of 2.5 L/min creates an inert atmosphere around the preform. During fiber drawing, the hole diameters are adjusted by applying pressure in the preform holes. Eventually, a cane is fabricated and drawn into a tube to obtain small core fibers.

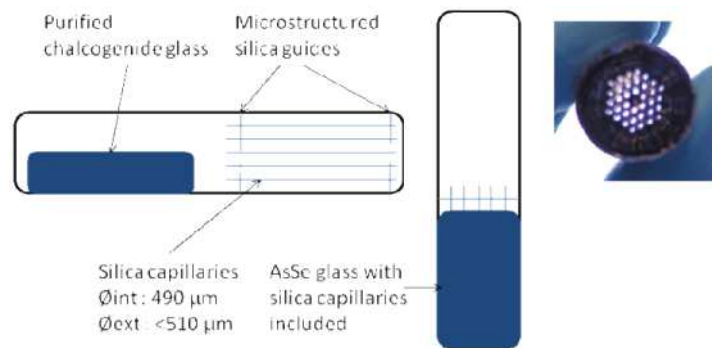


Fig. 1. Scheme of the silica mould. The glass is poured into the mould which is then removed by a HF treatment. The resulting preform is shown on the right picture.

2.4 Key points

The most important parameters are the size of the capillaries and the glass temperature during the pouring process. First, if capillaries are too thin, they break during the molding process. In contrary, we observed that if they are thicker than 15 μm , they create an important mechanical stress due to the difference between the thermal expansion of silica and As_2Se_3 [25, 26], inducing glass breaking. Secondly, the viscosity of the glass must be well chosen to the molding process. The glass is flowing into the cast with a low viscosity. Indeed, if the viscosity of the glass is too high, the glass does not flow into the mould, or it does not fill it. In the case of As_2Se_3 glass, the flowing temperature is around 420 $^\circ\text{C}$.

2.5 Geometries obtained

This casting method allows us to obtain various chalcogenide MOFs geometries. Indeed, the fibers can have 3 rings of holes (Fig. 2a, 2b) or a suspended core (Fig. 2c). The mode area can be controlled from 3 to 300 μm^2 . Fibers with very small core ($d=2\mu\text{m}$) can be obtained to enhance the nonlinear properties of the chalcogenide glass. Power delivery can also be considered with large core fibers (up to 20 μm diameter). The fiber can be either multimode or single mode, depending on the core size and the arrangement, the number and the size of

the holes [27]. The geometry is controlled and chosen to realize the desired optical functions. In the case of small core MOFs (Fig. 2b), we first stretch a 2 mm diameter cane from a microstructured preform. This cane is then inserted in a cladding made by a rotational casting method and is drawn into a fiber having a 2 μm core diameter [6]. Conversely, the large core fiber ($d=13 \mu\text{m}$) with a cladding made of 3 rings of holes (Fig. 2a) is fabricated in one step such as the suspended core fiber ($d=4 \mu\text{m}$) (Fig. 2c). In this last case, only 3 capillaries are used in the mould and the size of the holes is adjusted during the drawing.

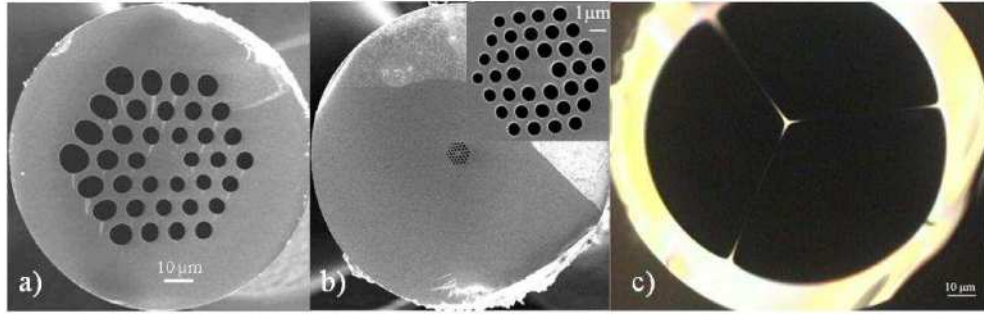


Fig. 2. a) SEM picture of a large core fiber. The core diameter is 13 μm . b) SEM picture of a small core fiber. The core diameter is around 2 μm . c) Optical microscopy picture of a suspended core fiber. The core diameter is 4 μm

3. Optical transmission

3.1 Large core

The high purification process used for the fabrication of As_2Se_3 rods induces very good material losses which are below 1 (± 0.2) dB/m in the wavelength range [1.6 μm – 2.8 μm] and below 0.5 (± 0.1) dB/m between 3 and 5 μm (Fig. 3a). The Se-H absorption band at 4.15 μm is removed and the O-H absorption band at 2.9 μm is kept around 3 dB/m in the best case.

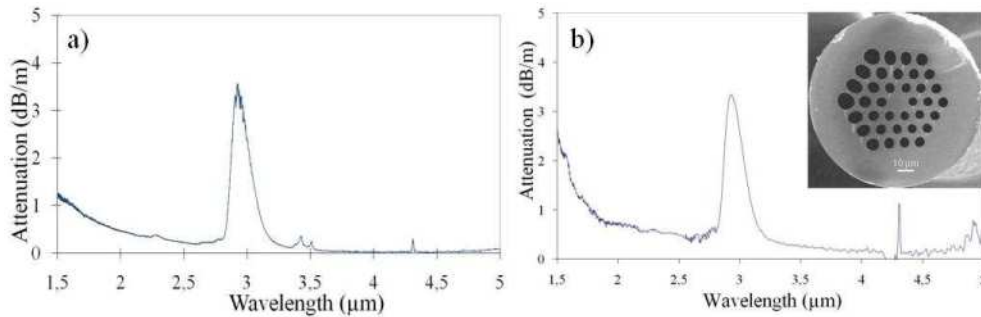


Fig. 3. a): Attenuation of the As_2Se_3 glass. b): Attenuation of the core of a multimode As_2Se_3 MOF.

The losses illustrated on Fig. 3b were measured on the fiber shown on Fig. 2a [28]. This fiber is multimode and does not show any bending losses for a bending radius of 2.5 cm. The losses on this multimode As_2Se_3 MOF were measured using a cut back method. The light is injected in 1.5 meter of fiber by a FTIR Nicolet and detected by a cooled InSb sensor. The injection spot size is about 1 mm^2 . The cladding modes are removed using GaSn alloy applied on the external surface of the MOF.

If we compare the losses of the glass with the losses of a MOF fabricated with the casting method, we can notice that the O-H absorption band has the same width and the losses are similar for the spectral range above 1.7 μm . The result indicates that the HF treatment does not affect the As_2Se_3 glass transmission. The absorption band at 4.3 μm is due to the variation

of carbon dioxide in the air during the cut back. (Fig. 3a and 3b). Losses are below $0.5 (\pm 0.1)$ dB/m in nearly the whole atmospheric window $3\text{-}5\ \mu\text{m}$, and between $0.5 (\pm 0.1)$ and $1 (\pm 0.2)$ dB/m from 1.7 to $2.7\ \mu\text{m}$. We observe that the losses for wavelengths higher than $1.7\ \mu\text{m}$ do not change from the raw material to the microstructured fiber.

3.2 Small core / Suspended core

For small core sizes, losses measurements are difficult with a good accuracy with the FTIR technology. Indeed, there is not enough light in the core to be detected by the sensor and we had to use a $1.55\ \mu\text{m}$ fibered diode laser. The cladding modes are removed with the same method used for large core fibers. For the suspended core fiber, we have measured losses to be around $4 (\pm 0.5)$ dB/m at $1.55\ \mu\text{m}$. Consequently, we can expect that lower losses can be achieved at $3.5\ \mu\text{m}$ due to the lower attenuation measured at these wavelengths (Fig. 3a and 3b).

Concerning the small core fiber illustrated in Fig. 2b, we have found that the 2-step fabrication process can induce some additional losses. Indeed, the cane quality decreases with time due to air exposure. The same cane was drawn twice, the first time briefly after the cane fabrication and the second time two months later. The losses at $1.55\ \mu\text{m}$ are respectively $4 (\pm 0.5)$ dB/m and $15 (\pm 1)$ dB/m.

4. Discussion

This casting method allows us to avoid the capillaries interfaces problems [19] and reduce considerably the fiber optical losses. However, we notice an increase of the losses for short wavelengths especially for the fiber made by the 2-step process, which is maybe due to some heterogeneous crystallization in the cane on the holes surface. In a second experiment, we have measured optical losses of a $13\ \mu\text{m}$ core fiber twice, one month apart, in the range $[1.5\ \mu\text{m}\text{-}5\ \mu\text{m}]$. The comparison of both attenuation spectra shows there is no evolution in time. These experiments let us think that the ageing problem probably comes from the cane drawing. We are studying the possibility of making such small core fibers in one step using larger preforms. These results also show that the water present in the air and the HF treatment don't affect the fiber loss. Indeed, the O-H absorption band does not increase with time even if there can be some surface oxidation due to air and visible light exposure [29, 30]. It seems likely that light and air can reach the holes of the cane as they are much larger ($d=65\ \mu\text{m}$) than in the large core fiber ($3\ \mu\text{m}$) which could explain the increase in light absorption at short wavelengths [29].

5. Conclusion

We have developed a new method to fabricate chalcogenide microstructured optical fibers using a whole silica mould. This method allows us to increase considerably the optical transmission of microstructured chalcogenide fibers, in particular in the $[3\ \mu\text{m} - 5\ \mu\text{m}]$ spectral band. Currently, the main limitation of this method concerns the small core fibers fabricated with a 2-step process. Nevertheless, suspended-core fibers with a core as small as $4\ \mu\text{m}$ have been obtained using the one step process. For this geometry, losses increase at wavelengths below $2\ \mu\text{m}$. One of the most reliable way to obtain IR supercontinuum is highly nonlinear, low loss, IR transparent microstructured optical fibers. As_2Se_3 suspended small core MOFs are good candidate to fulfill these requirements.

Acknowledgements

The authors want to thank the French Délégation Générale pour l'Armement for its financial support with the contract 07.34.031, the ANR FUTUR and the Mission des Ressources et Compétences Technologiques du CNRS for the project "18-08" CHALCOCAPIR.